Electrical transport and thermoelectric properties of Ni-doped perovskite-type $YCo_{1-x}Ni_xO_3$ ($0 \leq x \leq 0.07$) prepared by sol-gel process*

Liu Yi(刘 义)†, Li Hai-Jin(李海金), Zhang Qing(张 清), Li Yong(李 勇), and Liu Hou-Tong(刘厚通)

School of Mathematics and Physics, Anhui University of Technology, Ma'anshan 243032, *China*

(Received 13 October 2012; revised manuscript received 5 November 2012)

Electrical transport and thermoelectric properties of Ni-doped $YCo_{1-x}Ni_xO_3$ ($0 \leq x \leq 0.07$), prepared by using the sol-gel process, are investigated in a temperature range from 100 to 780 K. The results show that with the increase of Ni doping content, the values of DC resistivity of $YCo_{1-x}Ni_xO_3$ decrease, but carrier concentration increases. The temperature dependences of the resistivity for $YCo_{1-x}Ni_xO_3$ are found to follow a relation of $\ln\rho \propto 1/T$ in a low-temperature range (LTR) ($T <\sim 304$ K for $x = 0$; ~ 230 K $< T <\sim 500$ K for $x = 0.02$, 0.05, and 0.07) and high-temperature range (HTR) ($T >\sim 655$ K for all compounds), respectively. The estimated apparent activation energies for conduction E_{a1} in LRT and E_{a2} in HTR are both found to decrease monotonically with doping content increasing. At very low temperatures ($T <\sim 230$ K), Mott's law is observed for $YCo_{1-x}Ni_xO_3$ ($x \geq 0.02$), indicating that considerable localized states form in the heavy doping compounds. Although the Seebeck coefficient of the compound decreases after Ni doping, the power factor of $YCo_{1-x}Ni_xO_3$ is enhanced remarkably in a temperature range from 300 to 740 K, i.e., a 6-fold increase is achieved at 500 K for $YCo_{0.98}Ni_{0.02}O_3$, indicating that the high-temperature thermoelectric property of $YCoO_3$ can be improved by partial substitution of Ni for Co.

Keywords: perovskite cobalt oxides, sol-gel process, electrical transport, thermoelectric property

PACS: 72.15.Jf, 72.20.Ee, 72.80.Ga **DOI:** 10.1088/1674-1056/22/5/057201

1. Introduction

Perovskite-type rare earth cobaltites, including yttrium cobaltite, with general formula $RCoO_3$ (R = Y, rare earth), have attracted extensive attention in the last several decades due to the fact that they have potential technological applications in thermoelectric materials,[1–9] cathodes for solid oxide fuel cells (SOFC),[10,11] gas sensors,[12] and so on, and also have interesting, unusual, electrical and magnetic properties.[13–20] This performance oxide, as thermoelectric material, can be characterized by a dimensionless figure of merit ZT[21] ($ZT = PT/\kappa$, where T and κ are the absolute temperature and thermal conductivity, respectively; $P = S^2/\rho$ with S being the thermopower or the Seebeck coefficient, and ρ the electrical resistivity), is the power factor related to electrical property.[22] Therefore, large power factor and relatively low thermal conductivity are necessary for a high-performance thermoelectric material. As thermoelectric materials, these oxides have many advantages in addition to high thermal stability, oxidation resistance, and non-toxicity with respect to the traditional thermoelectric materials (e.g., Bi_2Te_3, PbTe), such as fairly large thermopower in the vicinity of room temperature (for instance, $S = 1050$ μV·K^{-1} at 300 K for $YCoO_3$,[14] $S = 555$ μV·K^{-1} at 300 K for $LaCoO_3$,[23] $S = 1300$ μV·K^{-1} at 300 K for $HoCoO_3$[24]) and small thermal conductivity (for example, $\kappa = 3.0$ W·m^{-1}·K^{-1} at 300 K for $La_{0.95}Sr_{0.05}CoO_3$[1]).

Among these oxides, the yttrium cobaltite ($YCoO_3$) was first synthesized by Demazeau *et al.*[25] Its crystal structure, thermoelectric (electrical and thermal), and magnetic properties have been widely investigated. Mehta *et al.*[26] and Knížek *et al.*[27] have reported that its crystal structure in a broad temperature range from 17 to 1000 K is a distorted perovskite structure with orthorhombic symmetry (space group *Pbnm* ($Z = 4$)), where each cobalt ion is surrounded by six oxygen atoms and only one form of cobalt site exists. Some physical properties of $YCoO_3$ were also reported by Knížek *et al.*[27] Moreover, the effects of element (e.g., Ca, Sr) doping in Y sites of $YCoO_3$ (e.g., $Y_{1-x}M_xCoO_3$ compounds with M = Ca, Sr) on its properties were also reported.[28–32] Among these studies, the thermoelectric properties of compounds $Y_{1-x}Ca_xCoO_3$, in which Ca atoms are partially substituted for Y atoms, were investigated by us, and it was found that Ca substitution for Y led to remarkable decrease in the electrical resistivity of $Y_{1-x}Ca_xCoO_3$,[26] but effective enhancement of its thermoelectric property.[29] At present, however, one knows little about how element doping in Co sites of $YCoO_3$ affect its properties. To our knowledge, no such kind of investigation as mentioned above has been performed

*Project supported by the Key Laboratory of Novel Thin Film Solar Cells, Chinese Academy of Sciences (Grant No. KF201101), the Key Science Foundation of Higher Education Institutions of Anhui Province, China (Grant Nos. KJ2011A053 and KJ2012Z034), and the National Natural Science Foundation of China (Grant Nos. 51202005, 11204005, and 41075027).

†Corresponding author. E-mail: yliu6@ahut.edu.cn

© 2013 Chinese Physical Society and IOP Publishing Ltd

so far. Therefore, it is interesting and very important to investigate the effects of element substitution for Co of $YCoO_3$ on its physical properties. In the present work, Ni-substituted compound $YCo_{1-x}Ni_xO_3$ is synthesized by a sol-gel process, and the influences of such doping on its DC electrical transport and thermoelectric properties are investigated in a temperature range from 100 to 780 K. The results indicate that electrical transport behavior of $YCoO_3$ is remarkably modified and its thermoelectric properties could be improved substantially by Ni substitution for Co of $YCoO_3$.

2. Experimental details

Nickel-doped yttrium cobaltates were prepared from stoichiometric yttrium, nickel, and cobalt nitrates. $0.02x$ ($x = 0$, 0.02, 0.05, 0.07) mol of $Ni(NO_3)_2{\cdot}6H_2O$ (98.0%), $0.02(1-x)$ mol of $Co(NO_3)_2{\cdot}6H_2O$ (99.0%), and 0.02 mol of $Y(NO_3)_3{\cdot}6H_2O$ (99.0%) were dissolved in 20 ml of an aqueous solution of 0.02 M citric acid (99.5%) confected by deionized water. The solutions were continuously stirred for about 1 h, resulting in a homogenization of Y^{3+}, Ni^{2+}, and Co^{2+} cations in the mixture solution. Subsequently, the mixtures were slowly heated to 90 °C, and at this temperature they were dried for 12 h, forming brown powders. The brown powders were calcined in air at atmospheric pressure in a muffle furnace at 300 °C for 2 h, forming black powder samples so as to remove organic compounds. Then, these powder samples were ground and subsequently compressed into pellets with 13 cm in diameter. Finally, bulk samples were obtained by sintering the green pellets in air and tube furnace at 900 °C for 120 h, followed by spontaneous cooling slowly down to room temperature in the furnace.

Phase structures and lattice constants for the obtained samples were determined by using XRD (Philips-X PERT PRO diffractometer) with Cu Kα irradiation at room temperature. The accurate lattice parameters were determined from the d-value of the XRD peaks using a standard least-squares refinement method with an Si standard for calibration. To measure their electrical resistivity, the bulk samples were cut into bar-shaped specimens, each with a size of about 12 mm × 2 mm × 1 mm. The electrical resistivity and the Seebeck coefficient were measured on a computer-assisted device. The DC electrical resistivity was measured in vacuum by a conventional standard four-probe method at temperatures ranging from 100 K to 720 K. The Seebeck coefficient was also measured in a vacuum in a temperature range from 300 K to 780 K. Carrier concentrations were determined by measuring the Hall coefficient at room temperature in a magnetic field $H = 0.73$ T.

3. Results and discussion

3.1. Phase determination, change of lattice parameters after Ni doping

Figure 1 displays the XRD patterns of $YCo_{1-x}Ni_xO_3$ ($x = 0$, 0.02, 0.05, 0.07). The diffraction peaks for synthesized $YCoO_3$ are indexed based on the standard JCPDS card (Card No. 88-0425) of $YCoO_3$, indicating that their main diffraction peaks are well accordant with each other. However, we should note that a small amount of impurity phase Y_2O_3 appears (as marked in Fig. 1) in our samples, which is consistent with the results in a previous synthetical work performed by Thornton *et al.*[13] For the synthesis of pure $YCoO_3$ phase, a high-pressure oxygen atmosphere is needed.[25] From Fig. 1, one can see that all the main diffraction peaks for the synthesized $YCo_{1-x}Ni_xO_3$ ($x > 0$) are the same as those for the synthesized $YCoO_3$, suggesting that Ni element has been doped into the lattice of $YCoO_3$, and the required phases of the doped compounds are formed. Moreover, to check whether the substitution of Ni for Co occurs, accurate lattice parameters (a, b, c) of $YCo_{1-x}Ni_xO_3$ with different Ni contents are calculated from the XRD data, and the results are plotted in Fig. 2. We see that the lattice parameters a, b and c for $YCoO_3$ are 5.1393, 5.4197, and 7.4588 Å, respectively, which are in agreement with the data measured by Mehta *et al.*[26] One can also see that with Ni content x increasing from 0 to 0.07, the lattice parameters a, b and c of $YCo_{1-x}Ni_xO_3$ increase from 5.1393, 5.4197, and 7.4588 Å for $x = 0$ to 5.1425, 5.4282, and 7.4662 Å for $x = 0.07$, respectively, indicating that the increase in lattice constant of $YCo_{1-x}Ni_xO_3$ is consistent with the doped content of Ni. These results also show that Ni replaces Co in $YCoO_3$ lattice and the substitutional compounds $YCo_{1-x}Ni_xO_3$ have been formed, for ionic radius of Ni^{2+} (0.69 Å) is larger than that of Co^{3+} (0.63 Å),[26] which will lead to lattice expansion upon doping. Moreover, Ni doping will give rise to lattice deformation (or distortion) of $YCoO_3$. In order to examine the deformation degree after substitution of Ni for Co, a geometrical quantity, Goldschmidt tolerance factor t is introduced, which is a fundamental parameter characterizing the degree of structural distortion in perovskite with the general formula ABO_3. It is defined as[33]

$$t = \frac{r_A + r_O}{\sqrt{2}(r_B + r_O)}, \tag{1}$$

where r_A, r_B, and r_O represent the average ionic radii of the respective cations (A and B) and oxygen, respectively. According to the data listed in Fig. 2, the relation $a < c/\sqrt{2} < b$ exists for all $YCo_{1-x}Ni_xO_3$ samples, indicating that they belong to so-called O-type structure,[14] and suggesting that the lattice deformation of $YCoO_3$ is relatively small after Ni substitution for Co. The dominating source of orthorhombic small distortion comes from buckling of the octahedral CoO_6 network, as

suggested elsewhere.[14] Owing to the effects of the experimental condition and the facts that the average ionic radius of A and O is invariable and the ionic radius of Ni^{2+} (0.69 Å) is larger than that of Co^{3+} (0.63 Å), the tolerance factors t will decrease as the Ni content x increases, suggesting that bucking of octahedral network of $YCo_{1-x}Ni_xO_3$ increases as the Ni content increases.

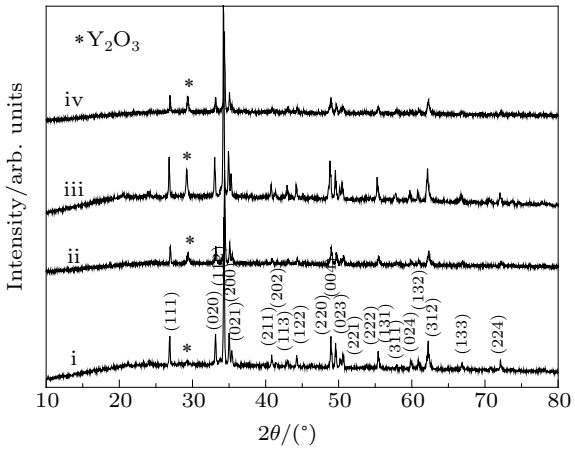


Fig. 1. XRD patterns (CuK$_\alpha$ irradiation) for $YCo_{1-x}Ni_xO_3$ (curve i: $x = 0$, curve ii: 0.02, curve iii: 0.05, curve iv: 0.07). The '*' denotes a little impurity phase.

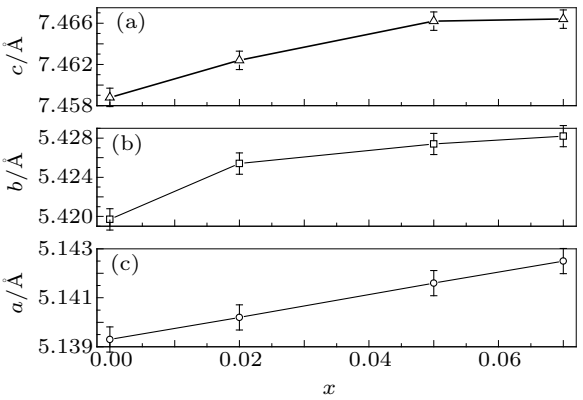


Fig. 2. Variations of the lattice parameters (a) a, (b) b, and (c) c with Ni content x for $YCo_{1-x}Ni_xO_3$ ($x = 0$, 0.02, 0.05, 0.07).

3.2. Effect of Ni doping on DC electrical resistivity

In Fig. 3, the temperature dependences of DC electrical resistivity ρ in the form of logρ for $YCo_{1-x}Ni_xO_3$ ($x = 0$, 0.02, 0.05, 0.07) compounds in a temperature range of 100–720 K are displayed. One can see that the electrical resistivity for $YCoO_3$ decreases with the increase in temperature in the whole temperature range measured, displaying semiconductor-like behavior. A similar phenomenon was also observed in other similar perovskite compounds, such as $LaCoO_3$.[34] After Ni substitution for Co in $YCo_{1-x}Ni_xO_3$ ($x > 0$), the temperature dependences of its resistivity appear not to change much. In other words, they still show semiconductor-like behaviors, i.e., $d\rho/dT < 0$. However, the absolute magnitudes of the electrical resistivity for $YCo_{1-x}Ni_xO_3$ at the same temperature decrease with the increase in Ni doping content. For example, the electrical resistivity of $YCo_{1-x}Ni_xO_3$ at 300 K decreases from 6.9 Ω·m for $x = 0$ to 1.9 Ω·m for $x = 0.02$, then decreases to 0.94 Ω·m for x=0.07 (see Table 1). The decrease in electrical resistivity for $YCo_{1-x}Ni_xO_3$ may mainly come from the contribution of carrier concentration. Table 1 lists the carrier concentration of $YCo_{1-x}Ni_xO_3$ at room temperature. We note that with the increase in Ni doping content x, the carrier concentration of $YCo_{1-x}Ni_xO_3$ increases, which is consistent with the change of lattice constant of $YCo_{1-x}Ni_xO_3$ shown in Fig. 2. For instance, the carrier concentration increases rapidly from 6.1×10^{14} cm^{-3} for $x = 0$ to 3.6×10^{16} cm^{-3} for $x = 0.02$, then it increases slowly from 1.6×10^{17} cm^{-3} for $x = 0.05$ to 2.6×10^{17} cm^{-3} for $x = 0.07$. This indicates that the decrease in the resistivity for $YCo_{1-x}Ni_xO_3$ is mainly due to the increase in carrier concentration since the substitution of Ni^{2+} for Co^{3+} should introduce acceptor levels in the energy gap. In addition, the carrier mobility is also listed in Table 1, with the aid of the formula $\mu = 1/\rho ne$, where μ, n, and e are the carrier mobility, carrier concentration, and electron charge, respectively. One can see that the carrier mobility decreases monotonically with Ni content x increasing, which may be caused by impurity scattering due to Ni doping. The values of carrier mobility μ for $YCo_{1-x}Ni_xO_3$ are relatively small because they are ceramic materials, which were also found in $Sr_{1-x}La_xPbO_{3-\delta}$ ($0 \le x \le 0.15$) with similar structures.[35]

Table 1. Values of room-temperature resistivity ρ_{rt}, carrier concentration n, and carrier mobility μ for $YCo_{1-x}Ni_xO_3$.

x	0.00	0.02	0.05	0.07
ρ_{rt}/Ω·m	6.9	1.9	1.1	0.94
$n/10^{18}$ cm^{-3}	6.1×10^{-4}	3.6×10^{-2}	1.6×10^{-1}	2.6×10^{-1}
μ/cm^2·V^{-1}·S^{-1}	10.4	0.91	0.35	0.26

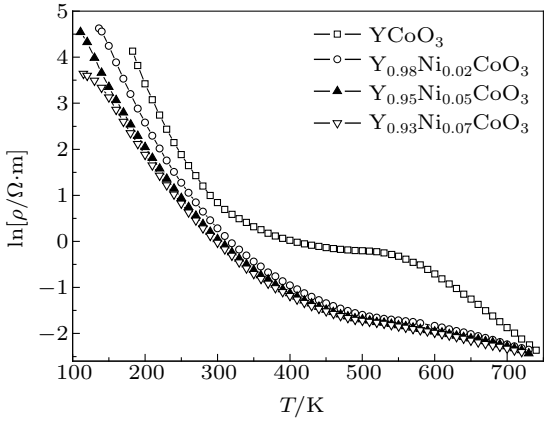


Fig. 3. Plots of the DC electrical resistivity lnρ versus temperature T for $YCo_{1-x}Ni_xO_3$ ($x = 0$, 0.02, 0.05, 0.07).

In order to examine temperature dependences of the electrical resistivity for $YCo_{1-x}Ni_xO_3$ in detail, the curves of resistivity ρ (in log) versus the reciprocal of temperature $1/T$ are

presented in Fig. 4. One can see that for each sample, there are two temperature regimes: low temperature range (LTR) ($T <\sim 304$ K for $x = 0$, ~ 230 K $< T <\sim 500$ K for $x = 0.02$, 0.05, 0.07) and high temperature range (HTR) ($T >\sim 655$ K for all compounds), within which good linear relations between $\ln\rho$ and $1/T$ exist, but they have different slopes in different temperature ranges. This indicates that the temperature dependences of the resistivity in LTR and in HTR (see the inset in Fig. 4) obey the following exponential (Arrhenius) law:[28]

$$\rho = \rho_0 \exp\left[\frac{E_a}{\kappa_B T}\right], \tag{2}$$

where ρ_0, E_a, and κ_B are the pre-exponential factor, the conduction activation energy, and the Boltzmann constant, respectively. By fitting the experimental data to formula (2) (see Fig. 4), one can obtain the activation energy E_{a1} in LTR and E_{a2} in HTR, as shown in Fig. 5. It can be seen from Fig. 5 that the activation energies E_{a1} and E_{a2} both decrease after Ni substitution: E_{a1} drops from 0.31 eV for $x = 0$ to 0.25 eV for $x = 0.07$, and E_{a2} drops from 1.2×10^{-3} eV for $x = 0$ to 3.3×10^{-4} eV for $x = 0.07$. Since $YCo_{1-x}Ni_xO_3$ is a p-type semiconductor system (which is proved by both a positive Hall coefficient and a positive Seebeck coefficient S), the exponential increase of the electrical resistivity with decreasing temperature would reflect the excitation of holes. Therefore, the decrease in the activation energy can be explained as a shift of the corresponding Fermi level E_F toward the edge of the valence band, making the energy difference between valence-band edge E_v and Femi level E_F, i.e., $E_a = E_F - E_v$, smaller. The E_{a2} in HTR is two orders of magnitude smaller than E_{a1} in LTR, which shows that there is a huge shift of the corresponding Fermi level E_F toward the edge of the valence band. Much more rapid decrease of E_{a2} than E_{a1} with Ni content increasing indicates that the deep level corresponding to E_{a2} is strongly influenced by Ni doping.

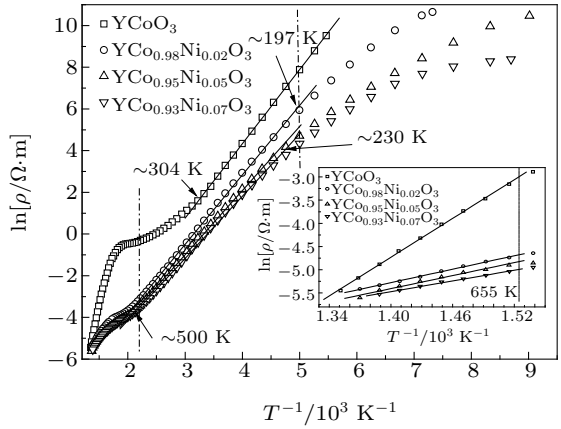


Fig. 4. Plots of $\ln\rho$ versus $1/T$ for $YCo_{1-x}Ni_xO_3$ ($x = 0$, 0.02, 0.05, 0.07). The inset shows the plots of $\ln\rho$ versus $1/T$ in high temperature range of $T >\sim 600$ K. The solid lines represent the best fitting of the experimental data to formula (2).

However, the temperature dependences of the resistivity for $YCo_{1-x}Ni_xO_3$ ($x \geq 0.02$) are found to follow Mott's law ($\ln\rho \propto T^{-1/4}$) if $T <\sim 230$ K for $x = 0.02$, 0.05, and 0.07, as shown in Fig. 6, suggesting that variable-range hopping conduction occurs in each of these compounds. According to Mott's variable-range hopping conduction theory, the relationship between resistivity and temperature can be expressed as[28,36]

$$\rho_{hop} = \rho_{hc} \exp\left[\left(\frac{T_0}{T}\right)^{1/4}\right], \tag{3}$$

with

$$T_0 = \frac{18.108\alpha^3}{\kappa_B N(E_F)}, \tag{4}$$

where ρ_{hc}, T_0, α, and $N(E_F)$ are a constant, the Mott characteristic temperature, the inverse decay length of the wave function for localized states near the Fermi level, and the density of localized states at Fermi level, respectively. By best fitting the experimental data using Eq. (3), we find that T_0 decreases rapidly from 1.63×10^9 K for $x = 0.02$ to 4.43×10^8 K for $x = 0.05$, and then decreases slowly to 4.29×10^8 K for $x = 0.07$. This decrease in T_0 may, according to Eq. (4), indicate that the density of localized states $N(E_F)$ increases with increasing doping content of nickel, which implies that stronger potential disorder is formed in the case of heavy doping.

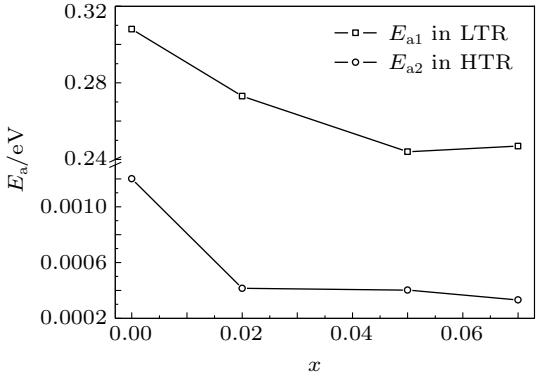


Fig. 5. Variations of activated energy E_a with Ni content of doping x in low-temperature (E_{a1}) and high-temperature (E_{a2}) regions for $YCo_{1-x}Ni_xO_3$ ($x = 0$, 0.02, 0.05, 0.07).

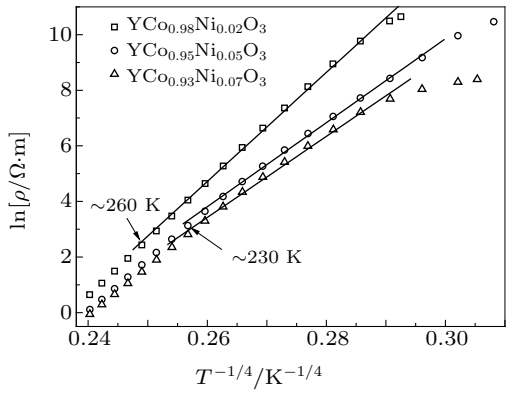


Fig. 6. Plots of $\ln\rho$ versus $T^{-1/4}$ for $YCo_{1-x}Ni_xO_3$ ($x \geq 0.02$). Solid lines: the linear fitting to the experimental data.

3.3. Effect of Ni doping on thermopower

Figure 7 shows the curves of Seebeck coefficient S of $YCo_{1-x}Ni_xO_3$ ($x = 0$, 0.02, 0.05, 0.07) versus temperature in a temperature range from 300 to 780 K. The positive values of the Seebeck coefficient in the whole temperature range measured for all samples suggest that the majority of charge carriers in $YCo_{1-x}Ni_xO_3$ are holes, which is also in accordance with our Hall measurements. The Seebeck coefficient of $YCoO_3$ first decreases slowly with the increase in temperature at $T <\sim 550$ K, then decreases rapidly as temperature increases further. This is consistent with the temperature dependence of its electrical resistivity. With the increase in Ni doping content x, the temperature dependence of the Seebeck coefficent for $YCo_{1-x}Ni_xO_3$ does not change remarkably. However, the absolute value of Seebeck coefficient decreases gradually. This phenomenon can be understood by the framework of Mott's model. By replacing electrical conductivity $\sigma(= en\mu(\varepsilon))$ in Mott formula[37,38]

$$S = \frac{\pi^2 k_B^2 T}{3e}\left(\frac{\partial \ln \sigma(\varepsilon)}{\partial \varepsilon}\right)_{\varepsilon=\varepsilon_F}, \tag{5}$$

we obtain

$$S = \frac{c_e}{ne} + \frac{\pi^2 k_B^2 T}{3e}\left(\frac{\partial \ln \mu(\varepsilon)}{\partial \varepsilon}\right)_{\varepsilon=\varepsilon_F}, \tag{6}$$

with

$$c_e = \frac{\pi^2 k_B^2 T}{3}\psi(\varepsilon), \tag{7}$$

where c_e, n, $\mu(\varepsilon)$, k_B, and $\psi(\varepsilon)$ are the electronic specific heat, carrier concentration, carrier mobility, Boltzmann constant, and the density of state (DOS), respectively. According to formula (6), the increase in carrier concentration should result in the decrease in the Seebeck coefficient. As mentioned above, our experiments indicated that Ni substitution results in substantial increase in carrier concentration, as shown in Table 1, which is qualitatively consistent with the decrease in the Seebeck coefficient for $YCo_{1-x}Ni_xO_3$ upon Ni doping.

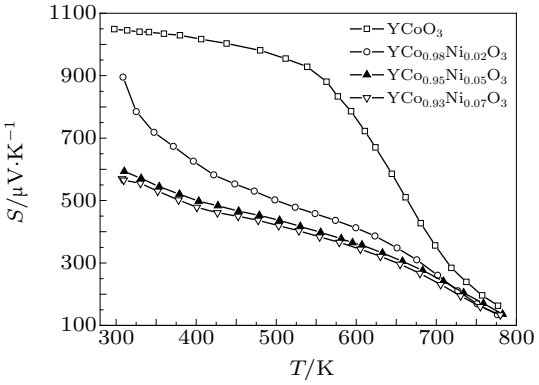


Fig. 7. Variations of the Seebeck coefficient S with temperature T for $YCo_{1-x}Ni_xO_3$ ($x = 0$, 0.02, 0.05, 0.07).

3.4. Effect of Ni doping on the power factor

Figure 8 shows variation of the thermoelectric power factor $P(= S^2/\rho)$ with temperature T for $YCo_{1-x}Ni_xO_3$ ($x = 0$, 0.02, 0.05, 0.07) in a temperature range from 300 to 720 K. The value of P is calculated by using the determined resistivity ρ and the Seebeck coefficient S shown in Figs. 3 and 7, respectively. We see that the power factor P of $YCoO_3$ increases slowly from 10^{-7} W·m^{-1}·K^{-2} at ∼300 K to 0.3×10^{-5} W·m^{-1}·K^{-2} at ∼600 K, then increases rapidly with the further increase of temperature. In contrast, the power factor P for $YCo_{1-x}Ni_xO_3$ ($x > 0$) increases sharply from 0.012×10^{-5} W·m^{-1}·K^{-2} at ∼ 300 K to 10^{-5} W·m^{-1}·K^{-2} at ∼ 500 K. Specifically, at 500 K, the power factor P increases from 1.49×10^{-6} W·m^{-1}·K^{-2} for $x = 0$ to 9.31×10^{-6} W·m^{-1}·K^{-2} for $x = 0.07$. This huge increase in P is mainly due to the decrease in the resistivity after Ni substitution for Co. The present results suggest that partial Ni substitution for Co in $YCo_{1-x}Ni_xO_3$ can substantially enhance high-temperature thermoelectric property of $YCoO_3$.

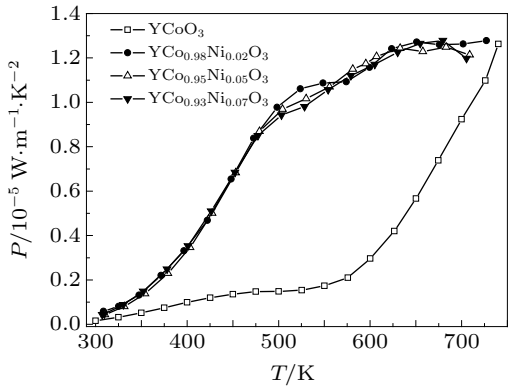


Fig. 8. Variations of the power factor P with temperature T for $YCo_{1-x}Ni_xO_3$ ($x = 0$, 0.02, 0.05, 0.07).

4. Conclusions

Nickel-doped cobalt oxides $YCo_{1-x}Ni_xO_3$ ($0 \le x \le 0.07$) are prepared by using a sol-gel process, and their electrical transport and thermoelectric properties are investigated in a temperature range from 100 to 780 K. The results show that with the increase in Ni content, the values of DC resistivity and Seebeck coefficient of $YCo_{1-x}Ni_xO_3$ decrease, which could be attributed to the increase in hole concentration, as evidenced by Hall measurements. The temperature dependences of the resistivity ρ for $YCo_{1-x}Ni_xO_3$ are found to follow a relation of $\ln\rho \propto 1/T$ in LTR ($T <\sim 304$ K for $x = 0$ and ~ 230 K$< T <\sim 500$ K for $x = 0.02$, 0.05, 0.07) and in HTR ($T >\sim 655$ K for all compounds), and both E_{a1} and E_{a2} are found to decrease monotonically with doping content increasing. At very low temperatures ($T <\sim 230$ K), Mott's law ($\ln\rho \propto T^{-1/4}$) is observed for $YCo_{1-x}Ni_xO_3$ ($x \ge 0.02$), indicating that considerable localized states are formed in the heavy doping compounds. Moreover, experiments show that the values of Seebeck coefficient S of $YCo_{1-x}Ni_xO_3$ decrease monotonically with the increase in Ni content x, presumably due to the rise of carrier concentration. The values of power

factor of $YCo_{1-x}Ni_xO_3$, however, are enhanced substantially in a temperature range from ~ 300 to ~ 740 K after Ni doping, indicating that the partial Ni doping in $YCo_{1-x}Ni_xO_3$ could improve the thermoelectric properties of $YCoO_3$ at high temperatures.

References

[1] Androulakis J, Pantelis M and Giapintzakis J 2004 *Appl. Phys. Lett.* **84** 1099

[2] Berggold K, Kriener M, Zobel C, Reichl A, Reuther M, Muller R, Freimüth A and Lorenz T 2005 *Phys. Rev. B* **72** 155116

[3] Zhang X, Li X M, Chen T L and Chen L D 2006 *J. Cryst. Growth* **286** 1

[4] Ji-Woong M, Won-Seon S, Hiroki O, Takasi O and Kunihito K 2000 *J. Mater. Chem.* **10** 2007

[5] Ji-Woong M, Yoshitake M, Won-Seon S and Kunihito K 2001 *Mater. Lett.* **48** 225

[6] Ohtani T, Kuroda K, Matsugami K and Katoh D 2000 *J. Eur. Ceram. Soc.* **20** 2721

[7] Kostogloudis G Ch, Vasilakos N and Ftikos Ch 1998 *Solid State Ionics* **106** 207

[8] Shang J, Zhang H, Li Y, Cao M G and Zhang P X 2010 *Chin. Phys. B* **19** 107203

[9] Wang H C, Wang C L, Zhao M L, Liu J, Su W B, Yin N and Mei L M 2009 *Chin. Phys. Lett.* **26** 107301

[10] Rossignol C, Ralph J M, Bae J M and Vaughey J T 2004 *Solid State Ionics* **175** 59

[11] Bansal N P and Zhong Z M 2006 *J. Powder Sources* **158** 148

[12] Emilio D and Carlos R M 2006 *Mater. Lett.* **60** 1613

[13] Thornton G, Morrison F C, Partington S, Tofield B C and Williams D E 1988 *J. Phys. C: Solid State Phys.* **21** 287

[14] Knížek K, Jirák Z, Hejtmánek J, Veverka M, Maryško M, Maris G and Palstra T T M 2005 *Eur. Phys. J. B* **47** 213

[15] Ding B F and Zhou S Q 2011 *Chin. Phys. B* **20** 127701

[16] Cai L G, Liu F M and Zhong W W 2010 *Chin. Phys. B* **19** 097101

[17] Bao J C, Zhang N, Cao H X and Geng T 2008 *Chin. Phys. B* **17** 317

[18] Feng J F, Huang Y H, Zhao J G, Han X F, Zhan W S, Zhao K and Wong H K 2005 *Chin. Phys.* **14** 1879

[19] Yu Z, Du Y W, Wang J H and Liu G Q 2004 *Chin. Phys.* **13** 90

[20] Liu X M, Yang M, Lu Z, Pei L, Liu J and Su W H 1999 *Chin. Phys.* **8** 690

[21] Arun M 2004 *Science* **303** 777

[22] Bhandari C M and Rowe D M 1995 *Optimization of Carrier Concentration* (Boca Raton: CRC Press)

[23] Zhou A J, Zhu T J and Zhao X B 2006 *Mater. Sci. Eng. B* **128** 174

[24] Bhide V G, Rajoria D S, Reddy Y S, Rama R G and Rao C N R 1973 *Phys. Rev. B* **8** 5028

[25] Demazeau G, Pouchard M and Hagenmüller P 1974 *J. Solid State Chem.* **9** 202

[26] Mehta A, Berliner R and Smith R W 1997 *J. Solid State Chem.* **130** 192

[27] Knížek K, Jirák Z, Hejtmánek J, Veverka M, Maryško M, Hauback B C and Fjellvåg H 2006 *Phys. Rev. B* **73** 214443

[28] Liu Y and Qin X Y 2006 *J. Phys. Chem. Solids* **67** 1893

[29] Liu Y, Qin X Y, Wang Y F, Xin H X, Zhang J and Li H J 2007 *J. Appl. Phys.* **101** 083709

[30] Michel C R, Gago A S, Guzmán-Colín H, López-Mena E R, Lardizábal D and Buassi-Monroy O S 2004 *Mater. Res. Bull.* **39** 2295

[31] Hejtmánek J, Jirák Z, Knížek K, Maryško M, Veverka M and Fujishiro H 2004 *J. Magn. Magn. Mater.* **272** e283

[32] Hejtmánek J, Jirák Z, Knížek K and Fujishiro H 2004 *Proceedings of the 2nd European Conference on Thermoelectrics of European Thermoelectric Society*, September 15–17, 2004 Kraków, Poland

[33] Zheng G H, Sun Y P, Zhu X B and Song W H 2006 *Solid Sate Commun.* **137** 326

[34] Yamaguchi S, Okimoto Y and Tokura Y 1996 *Phys. Rev. B* **54** R11022

[35] Hadjarab B, Bassaid S, Bouguelia A and Trari M 2006 *Physica C* **439** 67

[36] Xin H X, Qin X Y, Zhu X G and Liu Y 2006 *J. Phys. D: Appl. Phys.* **39** 375

[37] Xu G J, Ryoji F, Masahiro S, Ichiro M and Zhou Y Q 2002 *Appl. Phys. Lett.* **80** 3760

[38] Fisher B, Patlagan L, Reisner G M and Knizhnik A 2000 *Phys. Rev. B* **61** 470